*Wind and Structures, Vol. 3, No. 1 (2000) 11-21*
DOI: http://dx.doi.org/10.12989/was.2000.3.1.011


# Diffusion of passive contaminant from a line source in a neutrally stratified turbulent boundary layer

Albert F. Kurbatskii† and Sergey N. Yakovenko‡

*Institute of Theoretical and Applied Mechanics SD RAS, Physics Department, Novosibirsk State University, 630090 Novosibirsk, Russia*

**Abstract.** This paper presents results of modeling of the passive contaminant diffusion from a continuous line finite-size source located on the underlying surface of a neutral near-ground atmospheric layer obtained by using the non-local two-parameteric turbulence model and the transport equation of mean concentration. In the proposed diffusion model the turbulent diffusion coefficient changes not only with the vertical coordinate but also with the distance downstream from the source according to the experimental data. The results of the modeling reproduce structural features of the concentration field.

**Key words:** passive contaminant; turbulence; boundary layer.

## 1. Introduction

The transport equation for an averaged value of the passive contaminant concentration $C = < c >$ ($<\cdots>$ is statistical averaging) in a turbulent flow can be written in a closed form with the help of the gradient transport model for the turbulent substance flux vector ($K$-theory). In spite of its limitations usually associated with the locality of the gradient model for the turbulent scalar flux and with the dependence of the turbulent diffusion coefficient on the time of scalar emission from a source (Deardorff 1978), $K$-theory remains an attractive approximation due to its simplicity and because it allows to obtain fairly realistic results over a range of applications.

Fackrell and Robins (1982) obtained rather detailed measurement data for the concentration field of a passive contaminant spreading from finite size sources placed near the ground and elevated above the ground in the turbulent boundary layer initiated in the laboratory wind tunnel experiment. The vertical turbulent flux $<vc>$ can be calculated as $-K_y\,\partial C/\partial y$ for the near-ground source with the turbulent diffusion coefficient $K_y$ proportional to the turbulent viscosity coefficient $\nu_T$ ($\nu_T / K_y = \sigma_T =$ const, $\sigma_T$ is the turbulent Schmidt number). However, this has been demonstrated only for a single cross-section located at a distance of 2.5 boundary layer thickness downstream from the source. It has been justified because a typical length scale of eddies causing jet spreading is of the order or less than a typical jet size. For a finite size source elevated at 0.2 thickness of the boundary layer above the ground the measurements data show rough correspondence of locations where values of $<vc>$ and $\partial C/\partial y$ are maximum or zero. Therefore, the gradient transport model will also be appropriate for this case. Vertical profiles of the coefficient $K_y$ obtained from the measurements data

† Professor, Head and Chair of Aerophysics & Gasdynamics
‡ Senior Research Worker, Laboratory of Turbulence Modelling

(for distances from one to five thickness of the boundary layer downstream from the elevated source) indicate that the value $K_y$ increases with distance downstream from the source. The turbulent diffusion coefficient is found to be a function of a distance from the source since turbulent eddies in this case are not limited by the jet size. This behavior of $K_y$ corresponds to the results of Deardorff (1978).

Poreh and Cermak (1964) performed an experimental study of passive scalar diffusion of the ammonia gas from a near-ground line source in the boundary layer on a plane rigid surface. In these experiments, dynamics of contaminant jet evolution with the distance downstream from the source has been investigated in more detail. In particular, the turbulent diffusion coefficient has been found not only to be changing in the vertical direction but also to be an increasing function of the distance from the source.

In the present paper characteristics of the concentration field of a passive contaminant diffusing from a near-ground source in the turbulent boundary layer are evaluated. The simulation is based on the two-parameter model of turbulent transport. The turbulent kinetic energy (TKE) $E = 1/2<u_i u_i>$ and the spectral consumption $\varepsilon = \nu < (\partial u_i / \partial u_j)^2 >$ of the TKE ($\nu$ is the molecular viscosity coefficient) are defined by the differential transport equations. As a result, the turbulent viscosity $\nu_T \sim E^2 / \varepsilon$ and the turbulent diffusion coefficient $K_y$ are not only the functions of the vertical coordinate but they are also varying with the distance from the source which is in agreement with the experimental results discussed above.

## 2. Predictions of the velocity field based on the two-parameteric model of the turbulent transport

Existing variants of the $E$-$\varepsilon$ turbulent transport model differ mainly in the approximations of the turbulent diffusion terms in the governing transport equations and in various modifications of the $\varepsilon$ equation for flows near a wall (Nagano and Shimada 1995). This difference is caused by the absence of a natural boundary condition; the value of the dissipation rate $\varepsilon$ is finite on the rigid underlying surface. In the present paper the $E$-$\varepsilon$ turbulent transport model of Nagano and Tagawa (1990) is used allowing us to obtain acceptable results for turbulent quantities of the velocity field.

### *2.1. Governing equations for turbulent characteristics*

The turbulent transport model for the steady flow in the boundary layer along a smooth plate consists of

- the continuity equation,

$$\partial U / \partial x + \partial V / \partial y = 0 \tag{1}$$

- the equation for the longitudinal mean velocity $U$,

$$U\frac{\partial U}{\partial x} + V\frac{\partial U}{\partial y} = \frac{\partial}{\partial y}\left[(\nu + \nu_T)\frac{\partial U}{\partial y}\right] \tag{2}$$

- the equation for the TKE,

$$U\frac{\partial E}{\partial x} + V\frac{\partial E}{\partial y} = \frac{\partial}{\partial y}\left[\left(\nu + \frac{\nu_T}{\sigma_E}\right)\frac{\partial E}{\partial y}\right] + P - \varepsilon \tag{3}$$

- the equation for the spectral consumption of the TKE (the dissipation $\varepsilon$),

$$U\frac{\partial \varepsilon}{\partial x} + V\frac{\partial \varepsilon}{\partial y} = \frac{\partial}{\partial y}\left[\left(\nu + \frac{\nu_T}{\sigma_\varepsilon}\right)\frac{\partial \varepsilon}{\partial y}\right] + (C_{\varepsilon 1} f_1 P - C_{\varepsilon 2} f_2 \varepsilon)\frac{\varepsilon}{E} \tag{4}$$

In the Eqs. (1) - (4): $P = -\langle uv \rangle (\partial U / \partial y)$ is the turbulence production, $\langle uv \rangle = -\nu_T (\partial U / \partial y)$ is the shear Reynolds stress, and the eddy viscosity is

$$\nu_t = C_\mu f_\mu (E^2/\varepsilon) f_{LT} \tag{5}$$

$f_{LT} = \exp\{-\gamma [\delta(x) / (x - x_0)]^2\}$ at $x > x_0$ ($f_{LT} = 0$ at $x \le x_0$) is the intermittency function describing characteristics of the transition region from laminar to the turbulent flow state. Here $x_0$ is the coordinate of origin of the transition region, $\gamma = 10$ is the numerical coefficient; the boundary layer thickness $\delta(x)$ is defined as the coordinate $y$ at which $U/U_0 = 0.99$; $U_0$ is the mean velocity of the external flow.

$f_\mu = [1 - \exp(-y^+ / 26)]^2 \{1 + 4.1 / \mathrm{Re}_T^{3/4}\}$, $f_1 = 1$, $f_2 = [1 - \exp(-y^+ / 6)]^2 \{1 - 0.3 \exp[-(\mathrm{Re}_T / 6.5)^2]\}$

are the damping near-wall functions [5], $y^+ = (y u_*) / \nu$ is the non-dimensional near-wall coordinate in the direction normal to the wall, $\mathrm{Re}_T = E^2 / (\nu\varepsilon)$ is the turbulent Reynolds number, $u_* = \sqrt{\nu (\partial U / \partial y)_{y=0}}$ is the wall friction. In Eqs. (1)-(5) the standard values of coefficients are used: $\sigma_E = 1.0$, $\sigma_\varepsilon = 1.3$, $C_{\varepsilon 1} = 1.44$, $C_{\varepsilon 2} = 1.92$, $C_\mu = 0.09$.

The vertical component of the mean velocity vector in Eqs. (2)-(4) is calculated by integrating the continuity Eq. (1):

$$V = -\int_0^y (\partial U / \partial x) dy \tag{6}$$

Boundary conditions for the Eqs. (2)-(6) are as follows,

a) $y = 0$ : $U = E = 0$, $\varepsilon = \nu (\partial^2 E / \partial y^2)$;

b) $y \to \infty$ : $\partial U / \partial y = \partial E / \partial y = \partial \varepsilon / \partial y = 0$;

c) $x = x_0$ : the function $U = \sin[\pi y / (2y_0)]$ at $0 \le y \le y_0$ ($U = U_0$ at $y \ge y_0$) approximates the laminar Poiseuille profile ($y_0 = 0.002\, y_{\max}$ is the initial thickness of the laminar boundary layer); background values $E = 10^{-4} U_0^2$, $\varepsilon = 10^{-4} U_0^3 / y_{\max}$ are used for the TKE and the dissipation; height of the computational domain, $y_{\max}$, is the vertical scale taken to be equal to 127 cm (50 in) in order to resolve the last region of the concentration field evolution observed in the experiments of Poreh and Cermak (1964).

The parabolic Eqs. (2)-(4) together with the above boundary conditions are solved numerically by the implicit three-point finite-difference scheme and the running method. The computational grid along the vertical coordinate is non-uniform; its resolution increases toward the wall surface. The viscous sub-layer is explicitly resolved: at $y^+ \le 5$ there are five mesh intervals located along the $y$-axis in the region corresponding to the first cross section of the measurements (Poreh and Cermak 1964) with parameters $U_0 = 9$ ft/sec (= 274 cm/sec) and $\delta(x - x_0 = 34 \text{ ft}) = 7$ in. The number of nodes within the viscous sublayer increases in the positive $x$-direction. To verify the accuracy of the numerical solution computations have been performed on successive grids with resolutions differing by a factor of two in both $x$- and $y$- directions. As a result, a grid-independent solution has been obtained in the computational flow domain that includes ranges of coordinates of the laboratory

experiments (Poreh and Cermak 1964, Gibson *et al.* 1984, Klebanoff 1955) and those of the direct numerical simulation (DNS) of Spalart (1998).

### *2.2. Computational results of statistical characteristics of the velocity field*

In Fig. 1 the computed turbulent velocity field characteristics are compared with the data of Poreh and Cermak (1964), Gibson *et al*. (1984), Klebanoff (1955), Spalart (1998) at corresponding Reynolds numbers. Good agreement between the calculated mean-velocity profile and the measurements or DNS results is obtained in the external part of the boundary layer (Fig. 1a) where the profile deviates from the log law $U / u_* = \ln (y^+) / 0.41+5.0$ (dash-dot line 5 in Fig. 1a). Computed profiles of the shear turbulent stress (Fig. 1c,d) and the TKE (Fig. 1e,f) also agree with the experiment and DNS data, e.g., near a wall (Fig. 1c,e). Deviations of the computed TKE dissipation from the DNS results of Spalart (1988) in close proximity to the rigid surface (at $y^+ \le 20$) should be noted (Fig. 1g). It can be explained by the absence of the natural boundary condition for the function $\varepsilon$ on the wall. However, this difference does not significantly influence the computed second-order moments of the velocity field.

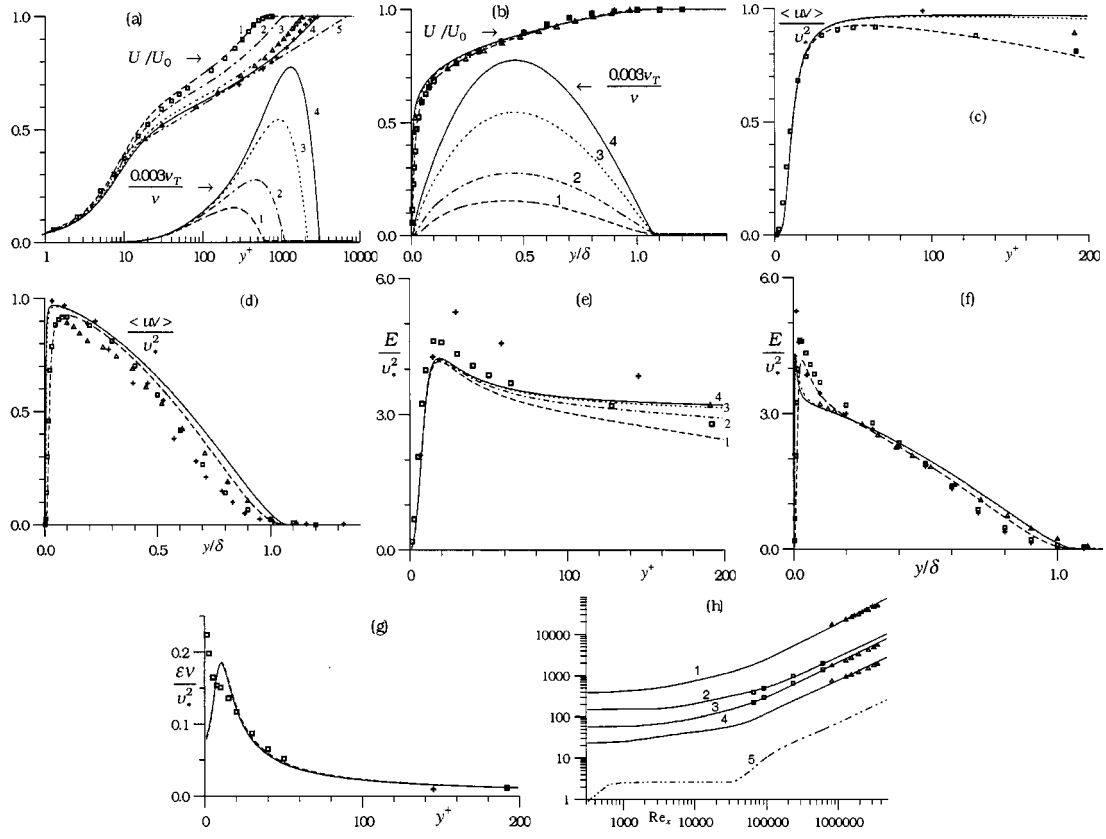


Fig. 1 Velocity field characteristics in the turbulent boundary layer
(a)-(g) □ [8], – – – $\mathrm{Re}_\theta = 1410$; △ [6], - - - - - $\mathrm{Re}_\theta = 5480$; + [7], —— $\mathrm{Re}_\theta = 7900$; (h) 1 - $\mathrm{Re}_\delta$, 2 - $\mathrm{Re}_{\delta 1}$, 3 -$\mathrm{Re}_\theta$, 4 - $\mathrm{Re}_*$, 5 - $0.003 \cdot \nu_t / \nu$ ; ★ - [3], △ - [6], □ - [8].

Fig. 1h shows the monotonic increase of the boundary layer parameters $\mathrm{Re}_\delta = U_0\delta/\nu$, $\mathrm{Re}_{\delta_1} = U_0\delta_1/\nu$, $\mathrm{Re}_\theta = U_0\theta/\nu$ $\mathrm{Re}_* = u_*\delta/\nu$ with the non-dimensional distance $\mathrm{Re}_x = U_0 x/\nu$. Here $\delta_1 = \int_0^\infty (1 - U/U_0)dy$ is the displacement thickness, $\theta = \int_0^\infty (U/U_0)(1 - U/U_0)dy$ is the momentum thickness. The maximum value of $\nu_t$ along the vertical cross-section also increases in the positive $x$-direction (Fig. 1h). These findings are confirmed by the measurements of Poreh and Cermak (1964) discussed in the Introduction. They can also be seen in Fig. 1a,b where the vertical profiles of $\nu_t$ are plotted by lines 1-4; the region corresponding to the parameters of experiments (Poreh and Cermak 1964, Gibson *et al.* 1984) is between lines 2 ($\mathrm{Re}_\theta$ = 2685) and 3 ($\mathrm{Re}_\theta$ = 5480).

## 3. Modeling of the concentration field dynamics

Applying the Eulerian approach can accurately solve diffusion problems in a real shear flow of the atmospheric boundary layer. The $C$ equation in the two-dimensional case is,

$$U\frac{\partial C}{\partial x} + V\frac{\partial C}{\partial y} = \frac{\partial}{\partial x}\left[D\frac{\partial C}{\partial x} - \langle uc\rangle\right] + \frac{\partial}{\partial y}\left[D\frac{\partial C}{\partial y} - \langle vc\rangle\right] \tag{7}$$

where $D$ is the molecular diffusion coefficient. For deriving the closed form of the Eq. (7) the turbulent contaminant flux vector components $<uc>$ and $<vc>$ are to be defined.

### *3.1. Transport equation for the mean contaminant concentration*

For the considered problem of passive scalar diffusion from the continuously working near-ground line source of assigned productivity $Q$ (Fackrell and Robins 1982, Poreh and Cermak 1964) in the steady turbulent flow of the near-ground layer the Eq. (7) can be written in the boundary-layer approximation as

$$U\frac{\partial C}{\partial x} + V\frac{\partial C}{\partial y} = \frac{\partial}{\partial y}\left[D\frac{\partial C}{\partial y} - \langle vc\rangle\right] \tag{8}$$

everywhere except in the immediate vicinity of the source. Fackrell and Robins (1982), Poreh and Cermak (1964) noted that it is difficult to obtain reliable experimental data for concentration field characteristics near the source. Following the measurements of Fackrell and Robins (1982), Poreh and Cermak (1964) the vertical turbulent flux $<vc>$ is parameterized by the gradient model with the turbulent diffusion coefficient $D_T$ ( = $K_y$) which is expressed in terms of the turbulent viscosity coefficient and the turbulent Schmidt number, $\sigma_T$ :

$$-\langle vc\rangle = D_T(\partial C/\partial y), \quad D_T = \nu_T/\sigma_T \tag{9}$$

Taking into account (9) the Eq. (8) becomes

$$U\frac{\partial C}{\partial x} + V\frac{\partial C}{\partial y} = \frac{\partial}{\partial y}\left[\left(\frac{\nu}{\sigma} + \frac{\nu_T}{\sigma_T}\right)\frac{\partial C}{\partial y}\right] \tag{10}$$

where $\sigma = \nu/D$ is the molecular Schmidt number. Distributions of the mean velocity vector components $U(x, y)$, $V(x, y)$ and the turbulent viscosity coefficient $\nu_t(x, y)$ are defined according to Eqs. (2)-(6). Similar to Eq. (10) has been used by Nieuwstadt and van Ulden (1978) to obtain mean concentration profiles in the near-ground layer which were in good agreement with the experimental data. The

vertical profiles of mean wind and the vertical turbulent diffusion coefficient were defined as functions of only of the vertical coordinate by using the similarity theory relations for the near-ground layer in the form obtained in the 1968 Kansas experiment.

The continuous near-ground passive-scalar line source of the strength $Q$ located at the point $x = x^*$ is determined by the contaminant conservation condition across the vertical section of the boundary layer. Integrating the Eq. (10) with respect to $x$ and $y$ and taking into account the continuity Eq. (1) and expressions (5), (9) for the turbulent viscosity and diffusion coefficients with the boundary conditions for $E$, $\varepsilon$ at $y = 0$, we have:

$$\int_0^{\infty}\{(CU)_{x=x_2}-(CU)_{x=x_1}\}dy=\int_{x_1}^{x_2}\left\{(D+D_t)\left(\frac{\partial C}{\partial y}\right)_{y=\infty}-D\left(\frac{\partial C}{\partial y}\right)_{y=0}-(CV)_{y=\infty}\right\}dx$$

Assuming $C = \partial C/\partial y = 0$ at $y \to \infty$ (the upper free-stream boundary) and $C = 0$ at $x = x_1$ (the region upstream from the source), the following integral equality is obtained,

$$\int_0^{\infty}(CU)_{x=x_2}dy=-\int_{x_1}^{x_2}D\left(\frac{\partial C}{\partial y}\right)_{y=0}dx=\int_{x_1}^{x_2}q(x)dx \tag{11}$$

Here the function $q(x)$ is a second-degree parabola in the form,

$$q(x) = A_0 + A_1(x - x^*) - A_2(x - x^*)^2 \tag{12}$$

for $(x^* - \Delta x^* \le x \le x^* + \Delta x^*)$ where $\Delta x^*$ is the half-width of the region through which the contaminant of the strength $Q$ is emitted into the boundary layer. Here the emission of the contaminant from the near-ground line source is assumed to be laminar and the range of parameters is the same as in the experiments of Poreh and Cermak (1964), i.e., the Reynolds number is $\mathrm{Re}_C = 3Q/(2\eta_C) \sim 10$ where $\eta_c$ is the dynamic contaminant viscosity.

The unknown coefficients in Eq. (12) are found from the conditions $q(x^* - \Delta x^*) = q(x^* + \Delta x^*) = 0$ and from the integral relation (11) which at $x_1 = x^* - \Delta x^*$ and $x_2 \ge x^* + \Delta x^*$ has the form

$$\int_0^{\infty}(CU)_{x=x_2}\,dy=\int_{x^*-\Delta x^*}^{x^*+\Delta x^*}q(x)dx = Q \tag{13}$$

The boundary conditions for the diffusion Eq. (10) are,

a) at $x = x^* - \Delta x^*$ (input data point in front of the source): $C = 0$;

b) at $y \to \infty$ (the upper free-stream boundary): $C = 0$;

c) at $y = 0$ :

$$\frac{\partial C}{\partial y} = -\frac{q(x)}{D} = \frac{3Q}{4\Delta x^*}\left[\left(\frac{x-x^*}{\Delta x^*}\right)^2-1\right]\le 0 \quad (\text{at } x^*-\Delta x^*\le x\le x^*+\Delta x^*) \tag{14}$$

$\partial_c/\partial y = 0$ (at the solid surface for $x \ge x^* + \Delta x^*$).

The Eq. (10) together with the above boundary conditions is solved numerically using the implicit three-point difference scheme. A number of $x$ steps in the interval $(x^* - \Delta x^* \le x \le x^* + \Delta x^*)$ is chosen so that the integral condition (13) is computed with the given precision at the vertical cross-section of the boundary layer, $x_2 = x^* + \Delta x^*$. The choice of the $x$ step for $x > x^* + \Delta x^*$ is based on the need to obtain a grid-independent solution in the computational domain which includes the range of coordinates of Poreh and Cermak's experiments and on the necessity to evaluate the condition (13) with the

given tolerance for $x_2 > x^* + \Delta x^*$.

### *3.2. Results of computation of the concentration field characteristics*

Computational results (lines) are compared in Figs. 2-4 with the measurements data [3] (markers) for the external flow velocity $U_0 = 9$ ft/s ( = 274 cm/s) for two series of experiments. In the Series I (S.I) the continuous line source of the strength $Q = 0.66$ mg/(cm·s) is placed on the underlying surface at the distance $x^* = 33.5$ ft ( = 1021 cm) from the turbulent boundary layer origin, and in the Series II (S.II) $Q = 0.55$ mg/(cm·s) and the distance is $x^* = 15.5$ ft ( = 472 cm). The limited length of the measuring section of the experimental set-up (Poreh and Cermak 1964) did not permit to perform measurements over the entire extension of the contaminant jet evolution for a fixed source position. The experimental data exists for the intermediate region of the scalar jet in the Series I and for the final zone in the Series II. It allows to establish some limit laws confirmed by the results of the

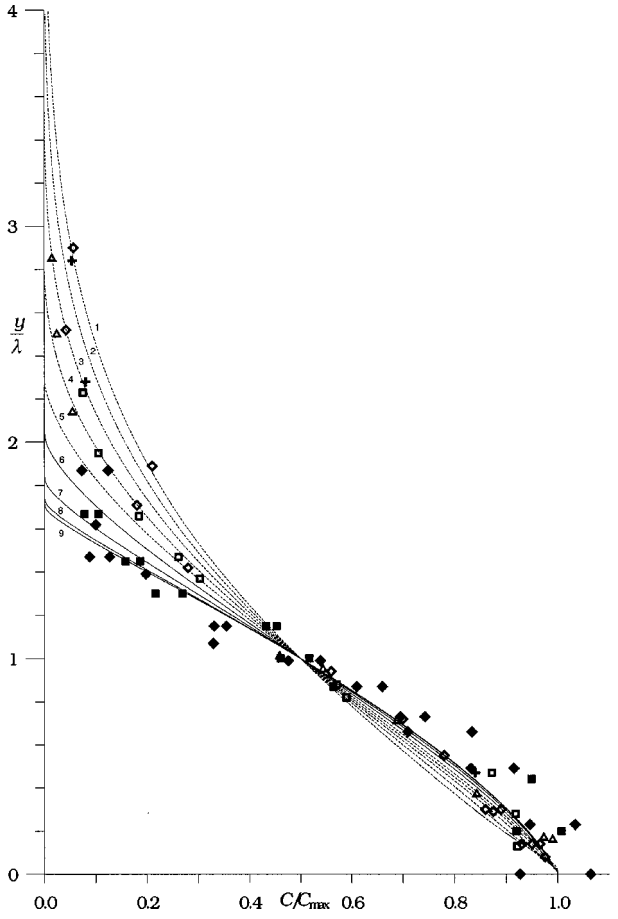


Fig. 2 Profiles of the mean concentration in different regions from a source: in the intermediate zone - S.I ($x^C$ = 3 ft - 1, ◇ ; $x^C$ = 5 ft - 2, + ; $x^C$ = 9 ft - 3, △ ; $x^C$ = 15 ft - 4, □ ); in the transitional zone - S.I ($x^C$ = 23.5 ft - 5), S.II ($x^C$ = 15 ft - 6 ; $x^C$ = 23,5 ft - 7) ; in the final zone - S.II ($x^C$ = 35.5 ft - 8, ◆ ; $x^C$ = 43.5 ft - 9, ■ ).

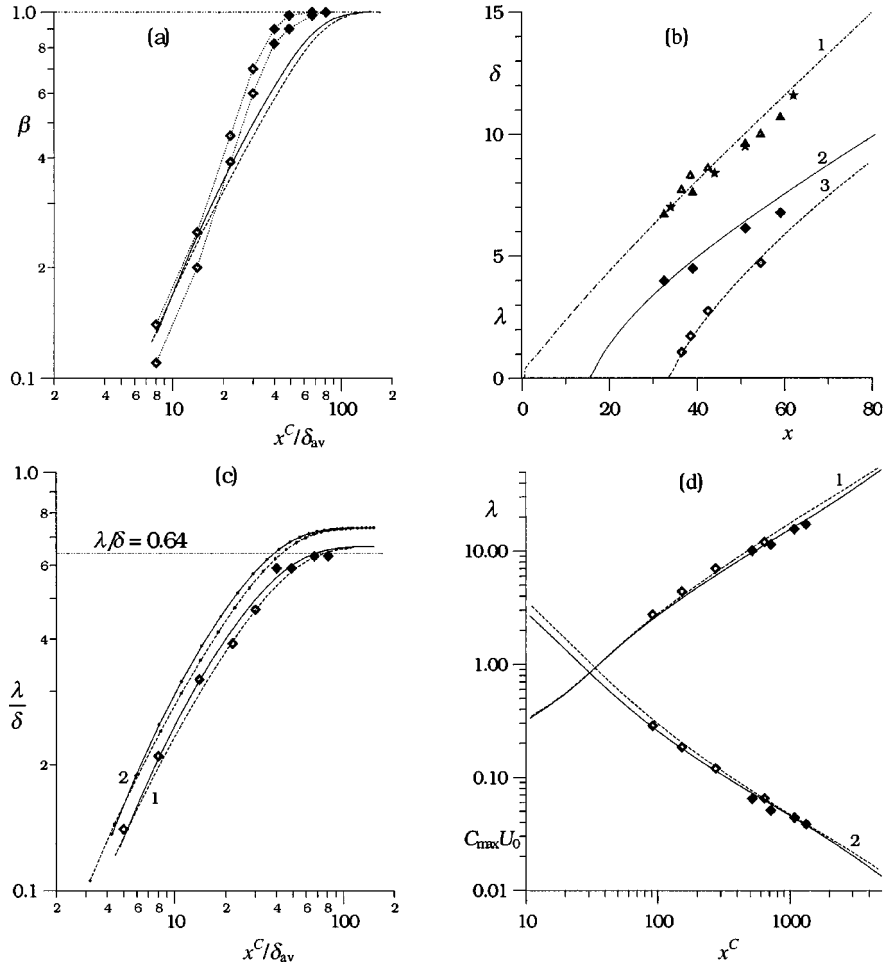


Fig. 3 Dependence of concentration field characteristics on the coordinate $x$ :
(a) parameter $\beta$ (lines ◇ ····· ◇ ··· ... ··· ◆ ····· ◆ ··· ◆ show the region of mean values of $\beta$ corresponding to those obtained in [3] from the measured points for $\delta(x)$ and $\lambda(x)$);
(b) thickness $\delta$ (lines 1, ★ are without the contaminant source, △ - S.I, ▲ - S.II ) and half-height $\lambda$ (2, 3, ◇ , ◆ ) in inches versus the distance $x$ in feet form the boundary layer origin;
(c) ratio $\delta / \lambda$ ;
(d) half-height $\lambda$ in cm (lines and markers 1) and the value of $C_{max}U_0$ in mg/(cm$^2$s) (lines and markers 2) versus the distance $x$ in cm from the source.
S.I - - - - - - - computation, ◇ measurement; S.II ———— computation, ◆ - measurement.

present paper.

Fig. 2 shows the dependence of the concentration profiles $C / C_{max}$ on the non-dimensional coordinate $y / \lambda$ , where $C_{max}$ is the maximum value of the mean concentration on the surface, $\lambda$ is the conventional thickness of the scalar jet defined by the value of $y$ under the condition $C(x, y = \lambda) / C_{max} = 0.5$. The computed profiles demonstrate the developing character of the concentration field. The diffusing contaminant jet is submerged entirely within the boundary layer. Its height is larger than the viscous sub-layer thickness ($\lambda >> \nu / u_*$). The parameter $\beta = L_\lambda / L_\delta$ ($L_\lambda = \lambda / (d\lambda / dx)$, $L_\delta = \delta / (d\delta / dx)$) characterizes a measure of the relative growth rates of the jet and the boundary layer thickness. This parameter is

small (Fig. 3a) in the near-source region where the diffusion of the passive scalar depends weakly on the growth rate of the boundary layer. Growth of the parameter $\beta$ with increase of the normalized distance $x^C / \delta_{av}$ from the source ($x^C = x - x^*$, $\delta_{av}$ is defined in (Poreh and Cermak 1964)) is followed by the transformation of the concentration field (lines 1-7 in Fig. 2). Predicted behavior of $\beta$ is in good agreement with the experimentally based conclusions of Poreh and Cermak (1964) about the dependence of diffusion field characteristics on the location of the source and on the distance from it, in particular about variation of the turbulent diffusion coefficient $D_T = \nu_T / \sigma_T$ not only with the height but also with the distance from the source. When the parameter $\beta$ increases, the contaminant jet evolution region approximately models the atmospheric diffusion from a near-ground source in the absence of buoyancy forces. It should be noted that the diffusion model reproduces correct power dependencies for growth of the scalar jet height $\lambda$ with the distance $x^C$ from the source (Fig. 3b-d) as does the model (2)-(6) of the velocity field for the boundary layer thickness $\delta$ (Fig. 3b). The rate of increase of the vertical jet size near the source is larger than the growth rate of the boundary layer thickness (Fig. 3b,c).

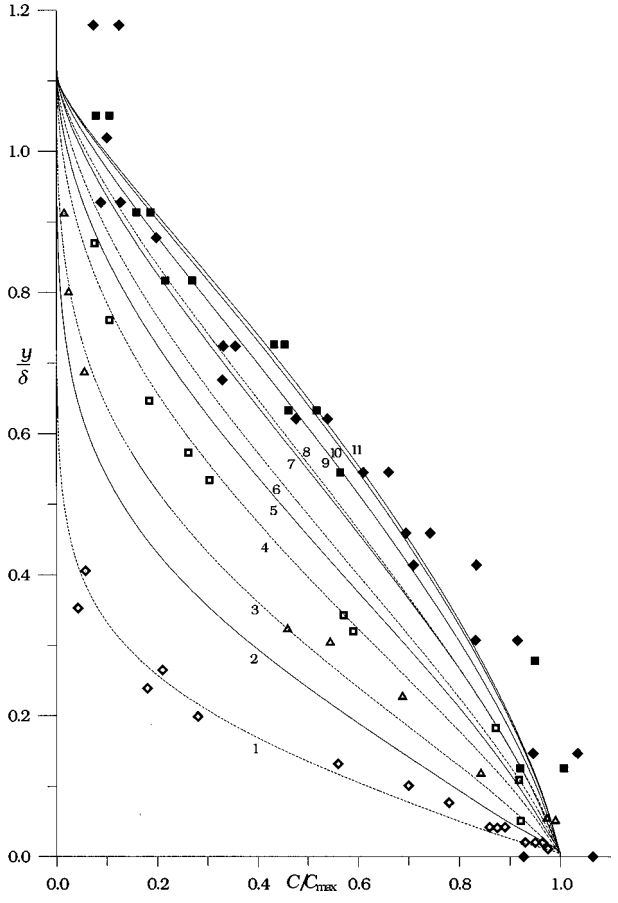


Fig. 4 Profiles of the mean concentration versus the vertical coordinate normalized by the boundary layer thickness
S.I: $x^C$ = 3 ft - 1, ◇ ; $x^C$ = 9 ft - 3, △ ; $x^C$ = 15 ft - 4, □ ; $x^C$ = 23.5 ft - 6; $x^C$ = 35.5 ft - 8.
S.II: $x^C$ = 3 ft - 2; $x^C$ = 9 ft - 5; $x^C$ = 15 ft - 7; $x^C$ = 23.5 ft - 9; $x^C$ = 35.5 ft - 10, ◆; $x^C$ = 43.5 ft - 11, ■.

In the final region the growth rates of vertical sizes of the boundary layer and the scalar jet tend to one power dependence so the parameter $\beta$ reaches the asymptotic value which is equal to one (Fig. 3a) and the ratio $\lambda/\delta$ asymptotically goes to 0.64 (Fig. 3c). Lines 1 in Fig. 3c and all lines in other Figures are obtained at $\sigma_T = 0.90$ and curves 2 in Fig. 3c are computed at $\sigma_T = 0.72$. For large values of parameters $x^C/\delta_{\text{av}}$ the dependence of diffusion field characteristics on the source location disappears gradually, and concentration profiles become approximately similar (lines 8, 9 in Fig. 2; lines 10, 11 in Fig. 4). It should be noted here that the developing boundary layer is not entirely self-similar. In particular, the boundary layer thickness $\delta$ and the typical length scale of the viscous sub-layer ($\sim \nu / u_*$) are described by different power dependencies on *x*. Therefore, characteristics of the passive-scalar concentration field vary together with the velocity field characteristics.

Transformation of the contaminant jet concentration field with changing the parameter $\beta$ from small values up to the asymptotic value of $\beta = 1$ is followed by the decrease of the maximum concentration on the underlying surface. Computational results show (Fig. 3d) that the functions $C_{\max}(x^C)$ and $\lambda(x^C)$ are not described by single power dependencies on the distance from the source at different values of $x^C$. It corresponds to the experimental observations discussed above. If the turbulent diffusion coefficient in the Eq. (10) depends only on the vertical coordinate (Kurbatskii 1993), then the predicted $C_{\max}$ behavior does not agree with the measurements data [3] given in Fig. 3d.

## 5. Conclusions

Modeling of the turbulent diffusion of passive contaminant in the boundary layer on a plane smooth underlying surface from a near-ground line source of the assigned strength has been carried out. The developed turbulent transport model includes the turbulent transport equations for the mean velocity, the turbulence kinetic energy, dissipation and mean concentration. The model reproduces characteristics of both the velocity field and the concentration field which are in good agreement with the experimental data and the results of direct numerical simulations. The experimental observations about the dependence of diffusion field characteristics on the distance from the contaminant source have been confirmed. It is found that the turbulent diffusion coefficient is a function of both the vertical coordinate and the distance downstream from the source. Power laws of variation of the typical vertical jet size and the maximum concentration on the underlying surface are not the same in different regions of the contaminant jet, which is consistent with the measurements of Poreh and Cermak (1964).

## Acknowledgements

The present work is supported by the Russian Fundamental Research Foundation Grant 99-05-64143.

## References

Deardorff, J.W. (1978), “Closure of second- and third-moment rate equations for diffusion in inhomogeneous turbulence”, *Phys. Fluids*., **21**, 525-530.

Fackrell, J.E. and Robins, A.G. (1982), “Concentration fluctuations and fluxes in plumes from point sources in a turbulent boundary layer”, *J. Fluid Mech*., **117**, 1-26.

Gibson, M.M., Verriopoulos, C.A. and Vlachos, N.S. (1984), “Turbulent boundary layer on a mildly curved

convex surface. Part 1: Mean flow and turbulence measurements", *Experiments in Fluids*, **2**, 17-24.
Klebanoff, P.S. (1955), "Characteristics of turbulence in a boundary layer with zero pressure gradient", *NACA Report* 1247.
Kurbatskii, A.F. (1993), "Turbulent diffusion of passive contaminant from a line source in the boundary layer", *Siberian Physical-Technical Journal* Issue 6 58-62. (in Russian)
Nagano, Y. and Shimada, M. (1995), "Computational modeling and simulation of turbulent flows", *Computational Fluid Dynamics Review 1995* / Eds. M. Hafez, K. Oshima. John Wiley and Sons: Chichester - New York - Brisbane - Toronto - Singapore, 695-714.
Nagano, Y. and Tagawa, M. (1990), "An improved $k$-$\varepsilon$ model for boundary layer flows", *Trans. ASME I: J. Fluid Engng*., **112**, 33-39.
Nieuswtadt, F.T.M. and van Ulden, A.P. (1978), "A numerical study on the vertical dispersion of passive contaminant from a continuous source in the atmospheric surface layer", *Atmospheric Environment*, **12**, 2119-2124.
Poreh, M. and Cermak, J.E. (1964), "Study of diffusion from a line source in a turbulent boundary layer", *Int. J. Heat Mass Transfer*, **7**, 1083-1095.
Spalart, P.S. (1988), "Direct simulation of turbulent boundary layer up to $R_\theta = 1410$", *J. Fluid Mech*., **187**, 61-98.

( *Communicated by Chang-Koon Choi* )